



OPEN Helium and argon cold plasma effects on the 4T1 cancer cells and a triple negative mouse model of breast cancer

Mahdiyeh Bakhtiyari-Ramezani^{1✉}, Meysam Nasiri² & Mansoureh Baniasadi³

Nowadays, cold atmospheric plasma (CAP) technology has developed as an innovative tool for cancer therapy. Although many studies have reported the antitumor effects of plasma *in vivo* and *in vitro*, there are many challenges, including standardization of plasma devices and treatment time for different tumors. For the first time, we aimed to evaluate and compare optimal exposure time and direction-dependent cellular effects of helium and argon plasma on the 4T1 cancer cells and a triple-negative mouse model of breast cancer. This study used two types of helium and argon plasma jet devices with different input parameters. *In vitro* evaluations on 4T1 cell line using the MTT assays and flow cytometry analysis demonstrate CAP-induced apoptosis in all treated groups, especially in the direct approach. These changes were concurrent with increased intracellular reactive oxygen species levels and decreased total antioxidant capacity in these cells. *In vivo* studies concurrent with *in vitro* results revealed that CAP therapy reduces tumor size, decreases Nottingham histological score, prevents weight loss, and increases the survival rate in all treated groups. These results suggest that plasma therapy may overcome the adverse effects of approved cancer therapeutic strategies and seems to be a significant issue for cancer patients in the clinical stage, alone or in combination with current therapeutic programs.

Keywords Non-thermal plasma, Cancer therapy, Breast tumor

Abbreviations

CAP	Cold atmospheric plasma
PAM	Plasma activated medium
OES	Optical emission spectroscopy
H&E	Hematoxylin and eosin
ROS	Reactive oxygen species
RNS	Reactive nitrogen species
RONs	Reactive oxygen and nitrogen species
NHG	Nottingham histopathological grading

According to statistics, there will be 297,790 new cases of invasive breast cancer diagnosed in American women. A lifetime risk of breast cancer is about 1 in 8 women and 1 in 833 men¹. Surgery is the first option for most solid tumors; however, complete removal of cancerous tissue is challenging, and residual microscopic or macroscopic tumors at the surgical site can lead to local regional recurrence. On the other hand, chemotherapy and radiotherapy have many side effects due to being non-selective^{2,3}. Therefore, less invasive and more selective therapeutic strategies are needed for tumor cell elimination. Plasma is an ionized gas containing free electrons, photons, ions, neutrals, and electromagnetic fields⁴. Due to the characteristics of plasma, it has wide applications, from generating energy⁵, food safety⁶, materials processing⁷, electronics⁸, and agriculture⁹ to medicine and biology¹⁰. The emerging application of plasma in biology consists of the sterilization of living and non-living surfaces¹¹, dermatology¹², wound healing¹³, tissue cutting¹⁴, dentistry¹⁵, blood coagulation¹⁶, and oncology¹⁷. The initial plasma applications in medicine have basically relied on thermal effects on the

¹Plasma Physics and Nuclear Fusion Research School, Nuclear Science and Technology Research Institute (NSTRI), Tehran, Iran. ²Department of Cellular and Molecular Biology, School of Biology, Damghan University, Damghan, Iran. ³Department of Biotechnology, Knowledge-Intensive Plasma Technology Development Company, Tehran, Iran. ✉email: mahdiyeh.bakhtiyari@gmail.com

surface of the biological target^{18–21}. Nowadays, non-thermal plasma can be produced at atmospheric pressure and room temperature^{22–28}, known as cold atmospheric plasma (CAP), and is supposed to be safe for biological application^{29–37}. Theoretically, any gas can be used to generate CAP. However, most of the literature has focused on using helium and argon because they produce stable plasma due to their monatomic nature, chemical inertness, and lower ionization potential^{38,39}. The results of these studies showed cytotoxic or growth-inhibiting effects of helium and argon plasma in various breast cancer cell lines and an animal model of breast cancer^{40–45}.

As a whole, plasma can target tumor cells in direct (direct exposure) and indirect (plasma-activated medium, PAM). In the direct approach, plasma directly interacts with targets. In contrast, in the indirect approach, a medium is activated by a plasma device, and then the activated medium is added to the target^{46–49}.

While numerous studies have documented the antitumor properties of plasma *in vivo* and *in vitro*^{50,51}, the therapeutic outcomes achieved with a specific plasma source cannot be directly extrapolated to another plasma device. This is attributed to the diverse range of biological effects elicited by the complex interplay of reactive species, radiation, electrical current flow, working gas flow, and heat transfer to the treated surface, which vary significantly depending on the plasma generation technology. Therefore, to avoid the risk of adverse effects such as toxicity, mutagenicity, or other harmful consequences, a comprehensive evaluation of the physical and biomedical performance parameters of each plasma device is imperative before its clinical application as a medical product. This study aimed to assess the optimal exposure duration and direction-dependent cellular effects of helium and argon plasma jet devices on 4T1 cancer cells and a triple-negative mouse model of breast cancer. Given that each configuration of plasma jets and their respective input parameters (such as power) generate a variety of reactive oxygen and nitrogen species (RONS), we focused our evaluation on the effects of helium and argon plasma on the 4T1 cancer cells by calculating the IC₅₀ values. Consequently, the investigation of the effects of plasma jets has not been performed under an identical setup.

Materials and methods

Configuration of CAP jet device

Helium and argon plasma jets produced by a Plasma Technology Development Company (Tehran, Iran) were used in this research. The plasma jets comprise the handpiece, the power supply, and the argon or helium gas cylinder. A plasma jet based on dielectric barrier discharge (DBDjet) produced helium plasma. A notable characteristic of this configuration is the lack of arc discharge, which facilitates the generation of cold plasma and medical applications. Figure 1A shows the details of the helium plasma jet. As shown in Fig. 1A, a high-voltage electrode made of stainless steel (inner diameter = 4 mm, thickness = 1 mm, length = 15 mm) is placed coaxially on the dielectric tube. The dielectric tube is made of quartz with an outer diameter of 4 mm and an inner diameter of 2 mm. As presented in Fig. 1B, the argon plasma jet is composed of a high-voltage rod-shaped electrode made of stainless steel (thickness = 0.1 mm) inside a quartz tube with an inner diameter of 2 mm and an outer diameter of 3 mm. The parameters and operating frequency of the argon plasma jet power source used

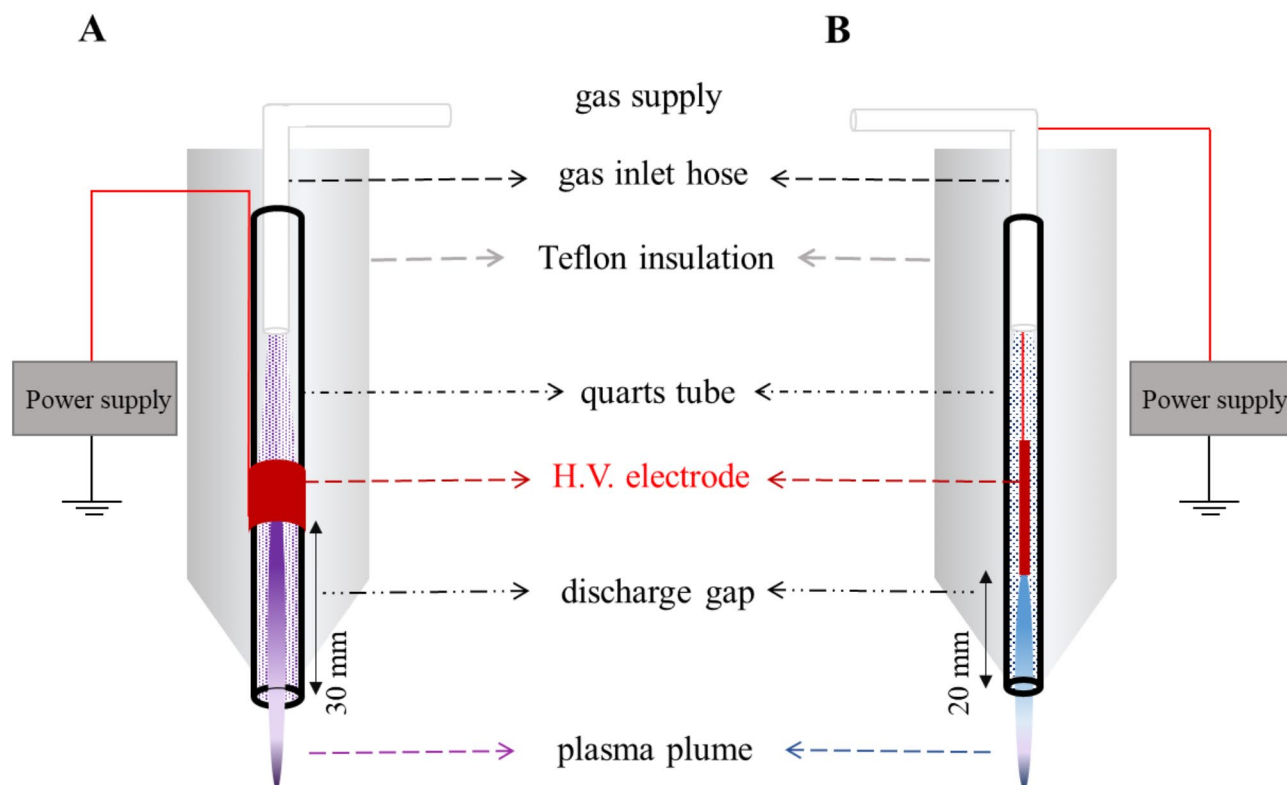


Fig. 1. Schematic cross-section of the (A) helium and (B) argon plasma jets.

in this research were carefully adjusted to prevent arc discharge. This precise calibration ensures that the system operates solely to produce micro discharge, thereby promoting a more stable and uniform configuration of the plasma jet. The helium gas was powered by an AC source at a voltage of 4.5 kV and a frequency of 20 kHz. The argon gas was powered by a pulse source at a voltage of 6 kV, a frequency of 50 kHz, and a duty cycle of 5%. A flow rate of 5 L per minute was set and controlled by a mass flow meter. An IR Thermometer (Fluke, US) monitored the CAP temperature on targets. The temperature was measured below 40 °C.

Optical emission spectroscopy measurement (OES)

The optical emission spectra of the argon and helium plasma jet devices were separately recorded using a single-channel spectrometer with a resolution of 0.6 nm manufactured by OPTC (Iran). The optical emission spectrum of each plasma jet was measured in the 200–980 nm range under ambient conditions using an optical fiber positioned 2 cm from the handpiece⁵².

Experimental design

This research was done in two sections: *in vitro* (cell line) and *in vivo* (animal model). Breast cancer induced by the 4T1 cell line is very similar to human breast cancer⁵³. This cell line is a triple-negative breast cancer (TNBC) molecular type. We know that molecular subtype, stage, and tumor location are key factors in therapeutic strategy selection⁵⁴. Unfortunately, inherent or developed resistance of breast cancer cells to chemotherapy, especially in the TNBC molecular type, hinders therapeutic efficacy in many cases^{55,56}, and more research is needed to find alternative or complementary therapies for this type of cancer.

Cell line part

Cell culture

The 4T1 cell line, a triple-negative mouse breast cancer cell line, was purchased from the Iranian Biological Resource Center (Tehran, Iran). The cells were cultured in a 6-well plate (BioFil, Spain) in RPMI-1640 Medium (Sigma-Aldrich, USA, R8758) supplemented with 10% fetal bovine serum (FBS) (Sigma-Aldrich, USA, F2442) and 1% Pen Strep (Thermo Fisher Scientific, Waltham, MA, USA) at 37 °C with 5% CO₂ and 95% humidity.

Plasma treatment of 4T1 cancer cells

Two general strategies were followed for CAP therapy. In the direct approach, the 4T1 cells were seeded in a 96-well plate (BioFil, Spain) at a density of 1×10^5 cells per well. After removing the medium, cancer cells in a well on a 96-well plate were covered by 20 μ L RPMI-1640 Medium. Then, the CAP jet was used to treat the cells vertically (Fig. 2A). In the indirect approach, 100 μ L of medium without cells was irradiated by plasma and then added to the cells seeded in 96-well plates at a density of 1×10^5 cells per well (Fig. 2B). According to the study design, five groups were defined as follows: (a) Control group of untreated 4T1 breast cancer cells; (b) The 4T1 cells treated with direct helium plasma; (c) The 4T1 cells treated with indirect helium plasma; (d) The 4T1 cells treated with direct argon plasma; (e) The 4T1 cells treated with indirect argon plasma. Based on our previous research, the tube-target distance was fixed at 2 cm⁵².

Cell viability assay

IC₅₀, or the half maximal inhibitory concentration, is a quantitative measure of the potency of a substance in inhibiting a specific biological process or response^{57,58}. Regarding chemotherapy drugs, the 50% inhibitory concentration is the anticancer drug concentration, causing a 50% reduction in cell viability. Determining the IC₅₀ dose is a fundamental aspect of preclinical and clinical pharmacology, contributing to the effective and safe use of chemotherapy drugs in cancer treatment^{59,60}. For IC₅₀ calculation, different substance concentrations are tested, and the degree of inhibition is measured. The resulting data generates a dose-response curve, and the IC₅₀ value is calculated using statistical methods^{59–62}. Given that differing durations of plasma exposure lead to varying concentrations of RONS, the IC₅₀ values were employed to investigate the optimal exposure time to achieve a 50% reduction in cell viability.

After 2 passages, cells were detached using 0.25% trypsin-EDTA (Life Technologies, USA). The 4T1 cells (at a density of 5×10^3 per well) were seeded into a 96-well polystyrene microplate (BioFil, Spain) with 100 μ L of culture medium per well. The cells were cultured for 24 h to ensure appropriate stability and cell adhesion. After removing the medium, dead cells were eliminated by a single wash with phosphate-buffer saline (PBS) (Sigma-Aldrich, USA, 806552), and fresh medium was added. For the IC₅₀ dose determination, cells were exposed to different plasma gases for 20, 40, 80, 160, and 320 s, using direct and indirect approaches. After that, cancer cells were incubated for 24, 48, and 72 h at 37 °C. To assess cell viability at these times, an MTT (3-(4,5-Dimethylthiazol-2-yl)-2,5-Diphenyltetrazolium Bromide) assay (DNAbiotech, DMA100) was conducted according to the manufacturer's protocol. After washing with PBS, 100 μ L of MTT solution was added, and cells were incubated at 37 °C in a humidified incubator with 5% CO₂ for 3 hours. Then, the MTT solution was removed, and 100 μ L of MTT solvent (0.4% (v/v) HCl in anhydrous isopropanol) was gently added to each well. All the measurements were done either after 10 min or within half an hour using a microplate reader (Spectrostarnano, Germany) at an absorbance of 570 nm, following 30 s of linear shaking. For accuracy, all of the measurements were repeated three times in triplicate.

Apoptosis and cell cycle analysis by flow cytometry

After treating cells with CAPs IC₅₀ doses, the 4T1 cells were incubated for 24 h, 48 h, and 72 h, based on cultivation time obtained from the MTT assay. Early and late apoptosis quantification was assessed using the Annexin V-FITC/PI apoptosis detection kit (Sigma-Aldrich, USA, CBA059), following the manufacturer's instructions. Briefly, CAP-treated cells were washed with PBS, resuspended in 100 μ L of binding buffer, and

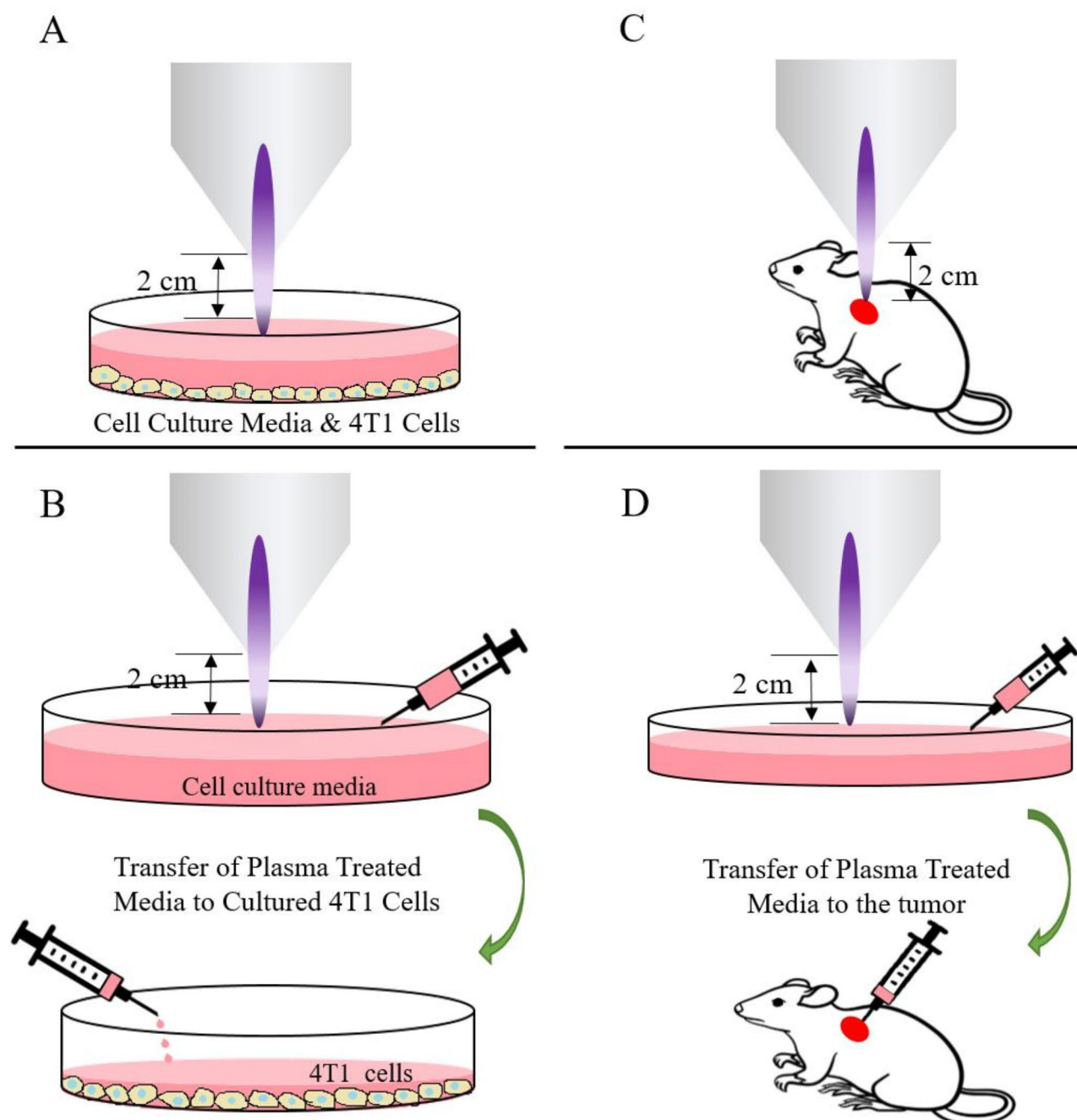


Fig. 2. (A, B) Schematic representation of direct and indirect CAP treatment in vitro, respectively, (C, D) Schematic representation of direct and indirect CAP treatment in vivo, respectively.

stained with 5 μ l FITC-conjugated Annexin-V for 15 min in darkness at room temperature. Then, cells were washed, resuspended in 250 μ l binding buffer, and incubated with 5 μ l Propidium Iodide (PI) (Sigma-Aldrich, MO, USA) for 10 min. Additionally, the DNA content was determined to quantify the G1, S, and G2/M phases of the cell cycle. Following treatment, the plasma-treated cells were separated using 0.25% trypsin-EDTA (Sigma-Aldrich, USA, T4049). After detachment, the cells were washed with PBS and fixed with ice-cold 70% ethanol for 2 h. Then, the cells were washed with PBS, treated with 50 μ g/ml RNase A (Sigma-Aldrich, USA, R6148) for 30 min, and incubated with Propidium Iodide. The results were analyzed using the BD FACSCalibur cytometer (BD Biosciences, San Jose, CA, United States).

Ferric ion reducing antioxidant power (FRAP) assay

Sample preparation

The 4T1 cells were harvested from the wells and centrifuged at 1500 rpm at 4 $^{\circ}$ C for 5 min. After discarding the supernatant, 200 μ l of Triton X-100 (Sigma-Aldrich, USA) was added to the cells, and the mixture was pipetted

and shaken for 30 min on ice. Then, the cells were lysed using a sonicator device (frequency 50 Hz, amplitude 80, half cycle per second) (Ultrasonic Technology Development Company, Iran). After that, the mixture was centrifuged for 15 min at 14,000 rpm at 4 °C, and the supernatant comprising the cell lysate was collected for future testing.

FRAP assay protocol

The FRAP assay method was performed to detect total antioxidant capacity (TAC). The FRAP reagent was prepared as follows: 300mM acetate buffer solution (ACS reagent, ≥99%, Merck, Germany, 236500), with a pH of 3.6, 10mM 2,4,6-tripyridyl-s-triazine (TPTZ) solution (Sigma-Aldrich, USA, T1253) in 40mM hydrochloric acid (Merck, Germany, H1758), and 20mM iron (III) chloride (Merck, Germany, 157740) were mixed in a 10:1:1 ratio. A 150μL of the FRAP reagent was mixed with 20μL of the sample, 20μL of ascorbic acid (Merck, Germany, A1300000) as a positive control, and 20μL of distilled water as a blank. The absorbance was measured using a microplate reader (Spectrostar nano, Germany) at an absorbance of 593 nm. The FRAP value was calculated using the following equation: $\text{FRAP value} = [(A1 - A0) / (Ac - A0)] \times 2$, where A1 is the absorbance of the sample, A0 is the absorbance of the blank, and Ac represents the absorbance of the positive control.

Reactive oxygen species (ROS) assessment

A fluorescence spectrophotometer (Perkin Elmer LS-55, USA) was used to assess the total ROS. Initially, a fresh solution of 2',7'-dichlorofluorescein diacetate (DCFDA) (ab-113851) was prepared in sterile Dimethyl sulfoxide (DMSO, Merck). The cancer cells were incubated with DCFDA at 37 °C for 45 min in the dark. To remove cell membranes, the mixture was centrifuged at 12,000 rpm for 30 min, and the sample's absorbance was measured at wavelengths of 488 and 593 nm.

Animal part

Laboratory animals

Twenty 8-week-old female Balb C mice weighing 20–25 g were purchased from the Pasteur Institute of Iran. The animals were kept in standard condition (light-dark cycle 12:12 h, temperature 22 ± 2 °C, and humidity 45–55%).

Breast tumor implantation

The 4T1 mouse model of breast cancer is a well-established model to mimic human mammary carcinoma, especially Stage IV triple-negative breast cancer⁶³. Cancer cells were cultured in RPMI-1640 Medium, enriched with 10% FBS and the antibiotics penicillin and streptomycin (1% pen/strep). Cells were maintained at 37 °C in 5% CO₂ under 90–95% humidity and subjected to sequential passages using trypsin (Gibco, Thermo Fisher Scientific Inc, Rockford, USA) and PBS. Animals were anesthetized by intraperitoneal (i.p.) injection of ketamine (Bremer Pharma, Germany) (100 mg/kg of body weight) and xylazine (Alfasan, Woerden, Holland) (10 mg/kg of body weight) mixture. For tumor induction, 5×10^5 cells were injected subcutaneously into mice at a total volume of 10μL. After 2 weeks, the animals were randomly divided into 5 groups ($n = 4$) as follows: (a) the control group (with no treatment), (b) the direct helium plasma-treated group, (c) the indirect helium plasma-treated group, (d) the direct argon plasma-treated group, and (e) indirect argon plasma-treated group. All animal protocols of this study were reviewed and approved by the Ethics Committee of Shahid Beheshti University of Medical Sciences (ethics code: IR.SBMU.CRC.REC.1401.039) under the ARRIVE guidelines.

CAP therapy in an animal model of breast cancer

Fifteen-day post-tumor induction, a single plasma therapy session was administered to the tumor region, either directly (Fig. 2C) or indirectly (Fig. 2D). The gas flow rate, exposure time, tube-target distance, and voltage of the CAPs jet were designated based on in vitro cell culture results. The duration of plasma therapy was determined based on IC 50 doses obtained from the MTT assay, and the tube-target distance was maintained at approximately 2 cm. In the direct approach, plasma was irradiated onto the tumor region at a constant frequency. In the indirect approach, plasma-activated media were injected into the center of the tumor at a dose of 50 μL. No significant temperature change was observed during the plasma treatment.

Tumor size and mice weight evaluation

Tumor size was measured using calipers on days 1 (pre-treatment) and 7 (post-treatment). Body weight was also monitored.

Histological evaluation

One day after the last plasma treatment, the mice were anesthetized via intraperitoneal injection of ketamine (50 mg/kg) and xylazine (5 mg/kg), then euthanized by cardiac exsanguination. The tumor tissue of all mice was separated and fixed with 10% formalin (Sigma-Aldrich, USA, HT501128). After 48 h, the steps of dehydration with alcohol, clarification with xylol, impregnation with paraffin (Bio Optica, Italy), molding, and then sectioning were performed. Hematoxylin-Eosin (QUELAB, Canada) staining was done, and slides were analyzed by light microscope (OPTICA, B-383Pl, Italy). The Nottingham Grading System was used to determine histological scores in breast tumors in all groups. The Nottingham histological grading score gives a score of 1 to 3 for each parameter: degree of mitosis, nuclear pleomorphism, and tubular formation. The final histological grade is based on a summation of the individual scores of the three parameters as follows: Grade 1 = the sum of the individual scores in Grade 1 is 3, 4, or 5; 6 or 7 in Grade 2; and 8 or 9 in Grade 3⁶⁴.

Statistical analysis

The statistical significance level was set at $p < 0.05$, and all data analysis was performed using SPSS Statistics 27.0, PRISM 9.5.1 (GraphPad software) and TIBCO[®] Statistica. Statistical analyses were performed on three replicates of data obtained from each treatment. Following the assessment of normality, the results were analyzed using analysis of variance, and the study presents descriptive statistics expressed as means \pm SD. The trends in mouse weight, tumor size, and the results of the plasma therapy test were evaluated through a two-way ANOVA repeated-measures analysis of variance followed by post-hoc Duncan testing. To analyze the variables among different study groups (TAC, ROC, cell cycle, histological score, and apoptosis), a one-way analysis of variance and Duncan post hoc test were utilized.

Results

In vitro results

OES assessment of CAP jets

Figure 3A, B shows the optical emission spectrum (OES) diagrams of helium and argon plasma jets. The presence of emission lines corresponding to the excitation of helium atoms⁶⁵ (characteristic helium peaks around 587 nm, 667 nm, 706 nm, and 728 nm) and argon⁶⁶ (the characteristic argon peaks as shown in Fig. 3B) confirms that gas ionization has occurred and plasma has been generated. A strong peak at approximately 309 nm⁶⁷, corresponding to hydroxyl (OH) compounds, is apparent in both diagrams; this indicates that such radicals are produced in the plasma environment of both jet devices. The appearance of a series of peaks in the 310–380 nm range in both diagrams is related to the excitation of nitrogen molecules, particularly the transitions of the second positive system (SPS)^{68,69}. In addition, the peaks related to the excitation of atomic oxygen appeared in both plasma jets. The visible peak at 777 nm in the helium plasma jet and 844 nm in the argon plasma jet confirmed the excitation of atomic oxygen⁷⁰. In the optical emission spectrum of the helium plasma jet, the peak at 285 nm is observed, which corresponds to nitrogen oxide (NO) species⁷⁰. The nitrogen oxide (NO) species are produced from reactions among radicals and active oxygen, and nitrogen species are generated through the interaction of plasma with ambient air. Also, hydrogen atoms may be produced by dissociating some hydroxyl (OH) radicals⁶⁵.

The effects of helium and argon plasmas on 4T1 tumor cell viability

MTT assay was performed to assess the best exposure time for helium and argon CAP therapy in direct and indirect approaches. The cancer cells were treated at five times of 20, 40, 80, 160, and 320 s, and cell viability was evaluated 24, 48, and 72 h after continuous culture following plasma exposure. The exposure times were selected based on our previous study⁵². Our data showed that the cell death rate is influenced by plasma exposure time and the duration after cultivation. Based on the calculated IC50 values, the optimal exposure times were 66.52 s at the 24-hour post-treatment time point, 110.6 s at the 48-hour post-treatment time point for indirect helium, 155 s at the 72-hour post-treatment time point for direct argon, 214.8 s at the 72-hour post treatment time point for indirect and indirect argon CAPs, respectively (Fig. 4). Based on these results, it can be concluded that direct helium plasma has a faster onset of action and induces cell death in a shorter exposure time. These data align with previous studies demonstrating the time-dependent cytotoxic effects of CAP on cancer cells.

Evaluation of early and late apoptosis and necrosis in 4T1 cells exposed to various CAPs

The effect of CAPs on early, late, and total apoptosis was measured by flow cytometry using annexin V-FITC/PI. The apoptosis rate of 4T1 cells significantly increased in all CAP-treated groups compared to the control group ($P < 0.001$). As shown in Fig. 5 and B, direct helium (54.96 ± 2.55) and direct argon CAPs (43.73 ± 3.89) induced more total apoptosis in 4T1 cells compared to the control group (4.68 ± 0.45), respectively. These results suggest that helium plasma exhibits a faster onset of action than argon plasma and demonstrates greater efficacy in inducing apoptosis in the 4T1 cancer cells. Interestingly, plasma has no significant effect on the rate of necrotic cell death.

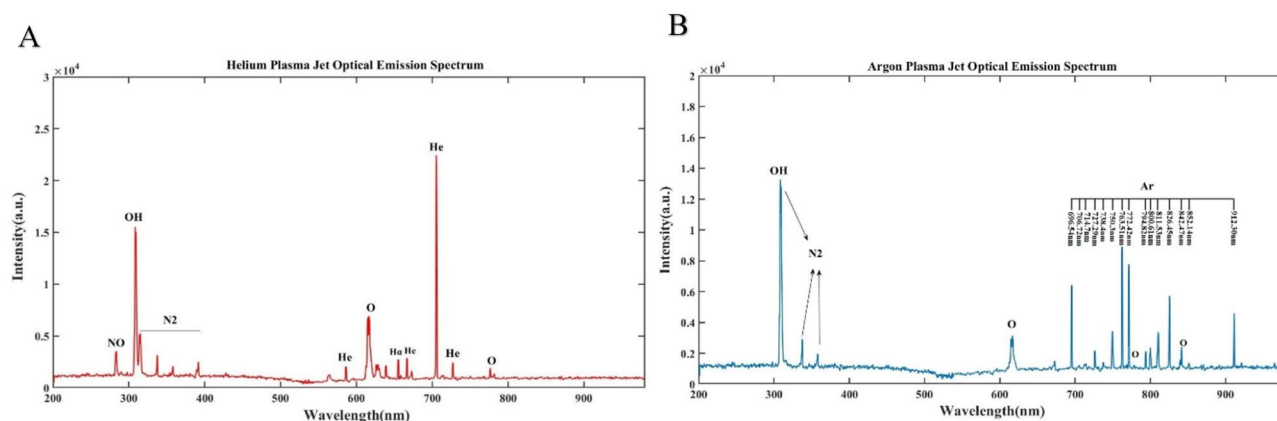


Fig. 3. Optical emission spectra of cold atmospheric(A) helium and (B) argon plasma jets.

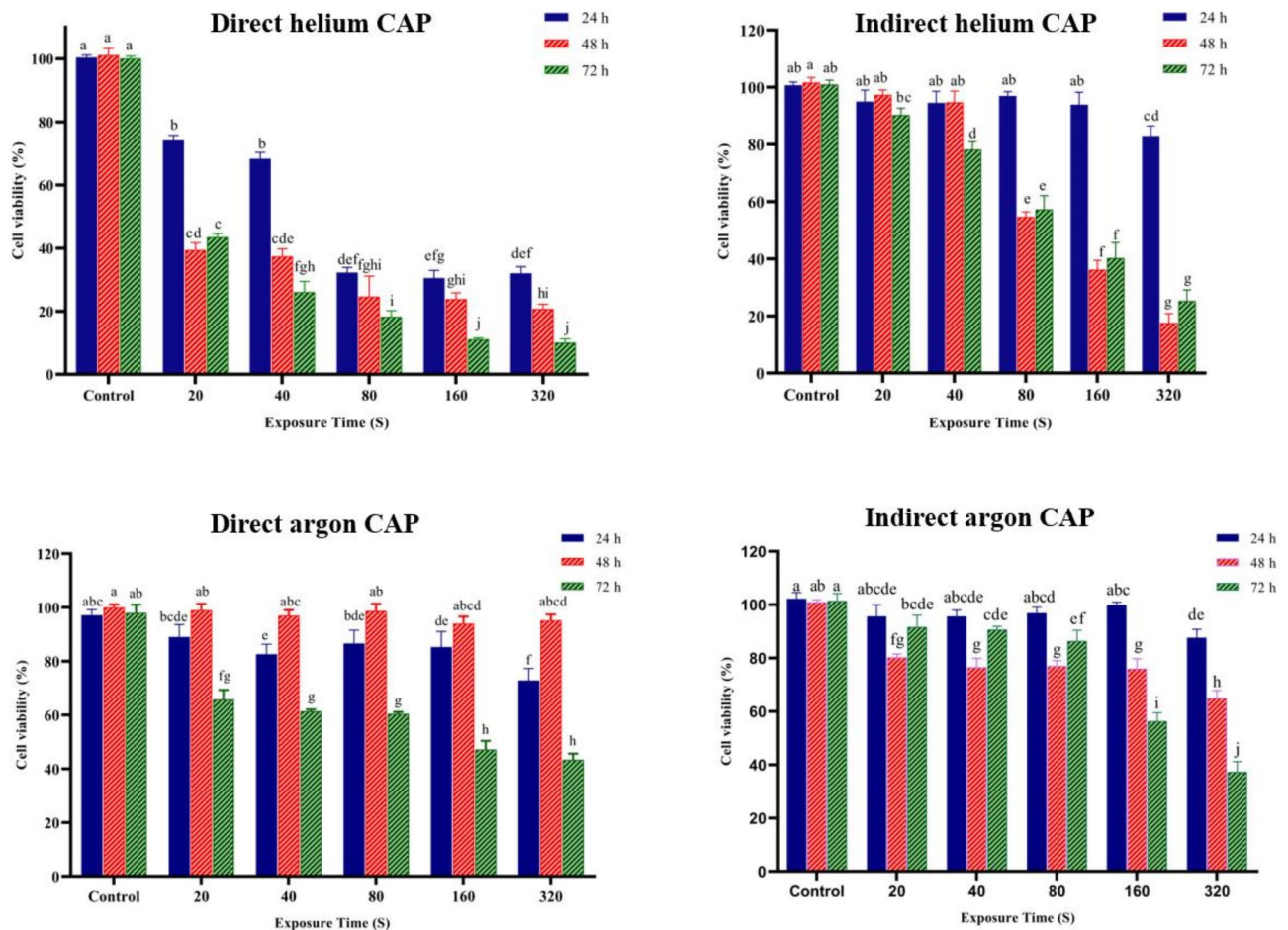


Fig. 4. Relative viability of 4T1 cells after treatment for 20, 40, 80, 160, and 320 s with different gas plasmas and 24, 48, and 72 h of culture after treatment with plasma. * Means followed by the same letter are not significantly different ($p < 0.05$).

Since failure in cell-cycle control contributes to cancer incidence, we studied the effect of plasma treatments on cell cycle progression in 4T1 cells. Fragmentation of internucleosomal DNA is accepted as one of the best-characterized biochemical markers of apoptosis. The sub-G1 phase is an abnormal phase in the cell cycle that is usually associated with the occurrence of apoptosis. As mentioned, we observed increased cell death in all treated groups. This increase in apoptotic cell death was correlated with a rise in the percentage of cells in the sub-G1 phase, especially in the direct helium (90.59 ± 1.88) and direct argon (83.9 ± 1.13) CAP groups compared to the control group (7.45 ± 0.65). In addition, CAP therapy significantly decreased DNA content in the G1 phase in all treated groups, especially in the direct helium CAP (3.85 ± 0.88) and direct argon CAP (6.31 ± 0.6) groups compared to the control group (80.44 ± 2.61), which can indicate the effects of plasma in preventing cells from entering the cell cycle and preventing cell division (Fig. 5C, D).

Total antioxidant capacity and reactive oxygen species level assessment in different CAP groups

The levels of intracellular ROS and TAC were analyzed to explore the possible mechanism of plasma therapy on 4T1 cancer cells. Plasma therapy significantly increased the concentration of reactive oxygen species, while TAC levels significantly decreased in all treated groups ($P < 0.001$). The highest increase in ROS was observed in the helium direct CAP (175 ± 6.24) and the argon direct CAP group (168.67 ± 4.51) compared to the control group (91.67 ± 7.64) (Fig. 6A). Although helium plasma produced higher levels of ROS compared to argon plasma, this difference was not statistically significant. The greatest decrease in TAC levels was also observed in the direct helium CAP (12.78 ± 0.44) and direct argon CAP (13.44 ± 1.16) groups, compared to the control group (19.09 ± 2.05) (Fig. 6B).

The effect of plasma therapy on tumor size in the different groups

To investigate the direct and indirect effects of helium and argon plasma on the tumor in vivo, the size of the tumor was measured on the first day (before treatment) and after seven days (after the last treatment). As observed in Fig. 7A and B, while the tumor size increased in the control group (2753 ± 349.11) on the seventh day, a single CAPs treatment prevents breast tumor growth in all treated groups, especially in the direct helium (687.25 ± 118.88), and direct argon (505.5 ± 18.07) CAP groups. While the direct argon plasma-treated group

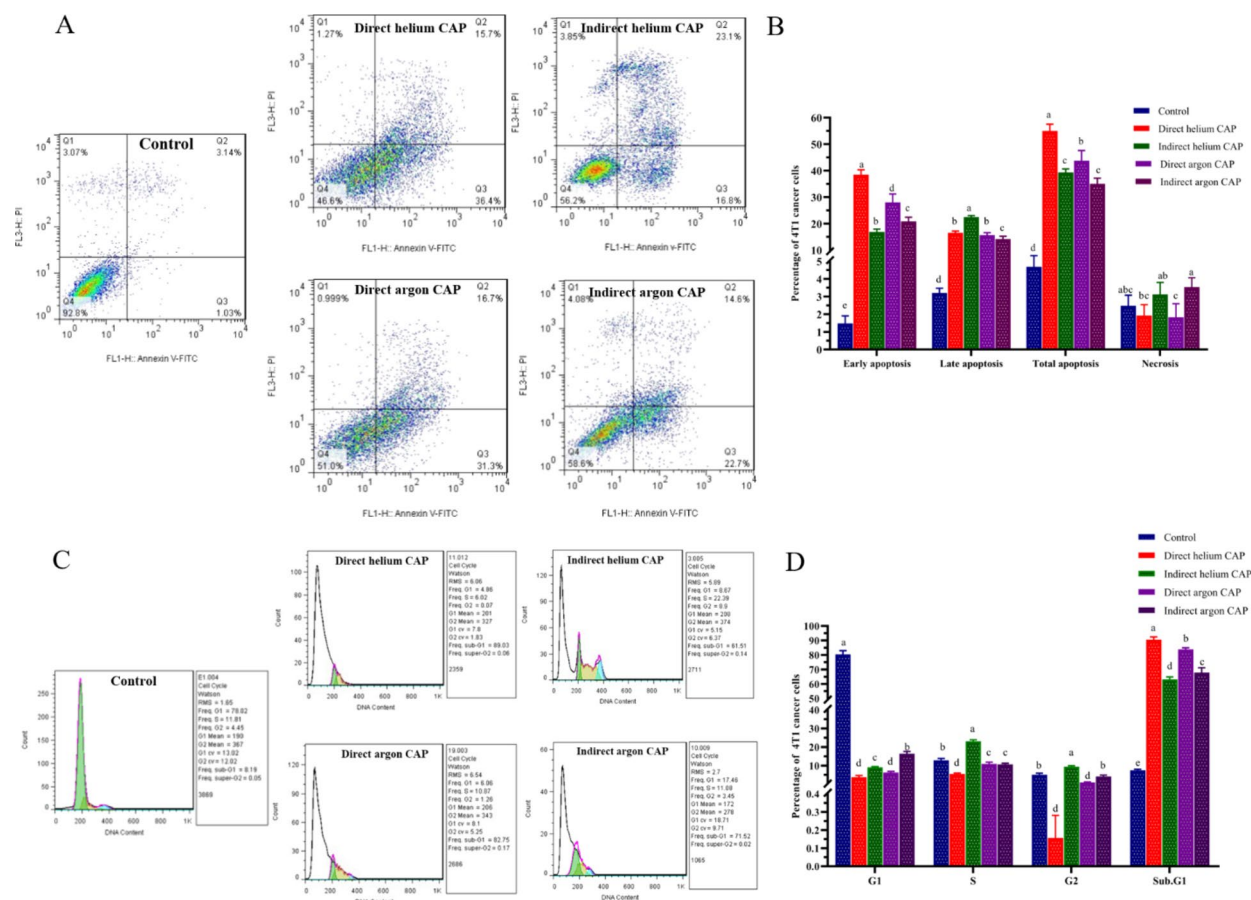


Fig. 5. (A) Flow cytometry analysis using the Annexin V/PI staining technique. The lower left quadrant represents living cells, the upper left quadrant shows the necrotic cell population, the lower right quadrant depicts early apoptotic cells, and the upper right quadrant represents late apoptotic cells. (B) Quantitative plot of flow cytometry data. Comparing the rate of apoptosis and necrosis of 4T1 cells due to CAP therapy. (C) Evaluation of cell cycle distribution in response to various plasma jet treatments. (D) A quantitative comparison of the CAPs effect on the proportion of cell cycle arrest in 4T1 cells. * Means followed by the same letter are not significantly different ($p < 0.05$).

exhibited a greater tumor size reduction than the direct helium group, this difference was not statistically significant.

The effects of plasma jets on the animal weight

As shown in Fig. 8, the animal weight in the control group on day 7 significantly decreased compared to day in the control group, and plasma therapy prevents weight loss in all studied groups.

The effects of plasma jets on animal survivability

Kaplan-Meier analysis showed that plasma therapy significantly increased the median survival of animals compared to the control group (Fig. 9). The highest survival rate was observed in the direct helium (56 ± 0) and direct argon CAP (50.33 ± 5.67) groups compared with the control group (30.17 ± 5.90). While the survival time in the direct helium plasma-treated group was longer than that of the direct argon plasma-treated group, this difference was not statistically significant.

H&E staining of tumor tissues

Hematoxylin and Eosin (H&E) staining was done to determine histological scores in breast tumors in all groups. As shown in Fig. 10A, most of the cells had high proliferation and were mainly in the mitosis phase, which indicated the high activity of tumor cells in the control group. However, the cell proliferation rate decreased in all CAP-treated groups. Overall, the results showed that plasma therapy caused a significant decrease in the degree of mitosis, nuclear pleomorphism, and tubular formation, defined as Nottingham's histological score, compared to the control group (Fig. 10B). The most significant reduction in histological score was observed in the direct helium and direct argon groups, with no significant difference between them. Furthermore, angiogenesis and, as a result, blood supply decreased in the treated groups compared with the control group (Fig. 10A).

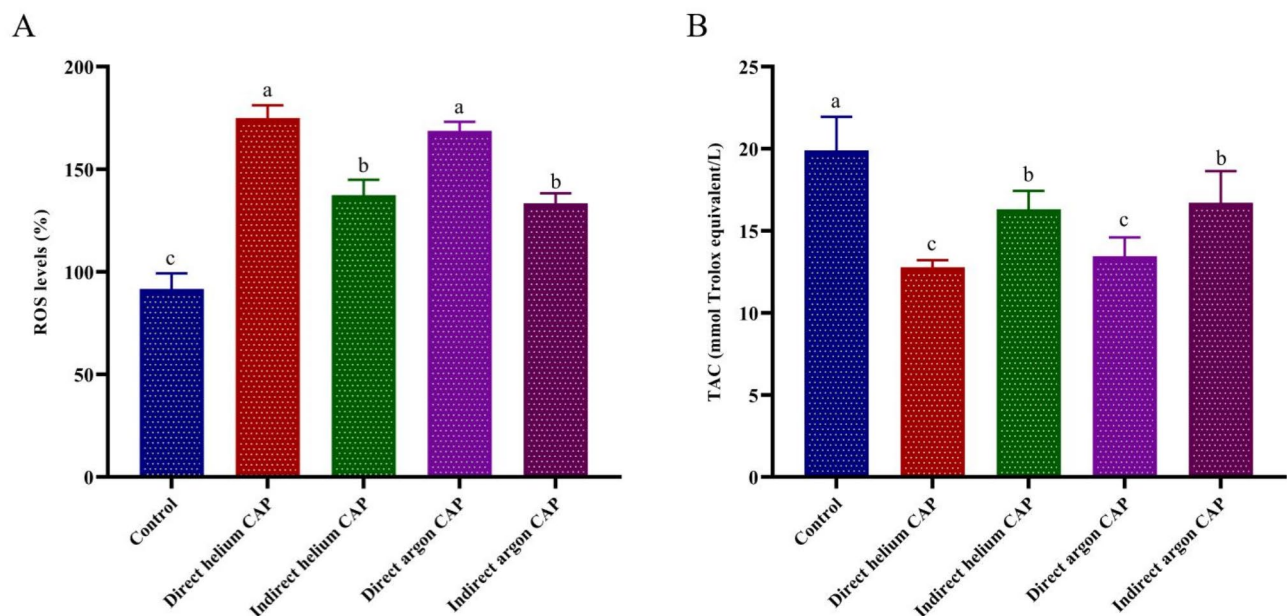


Fig. 6. (A) Evaluation of the reactive oxygen species level (ROS), and (B) The total antioxidant capacity (TAC) in 4T1 cells exposed to different CAPs. * Means followed by the same letter are not significantly different ($p < 0.05$).

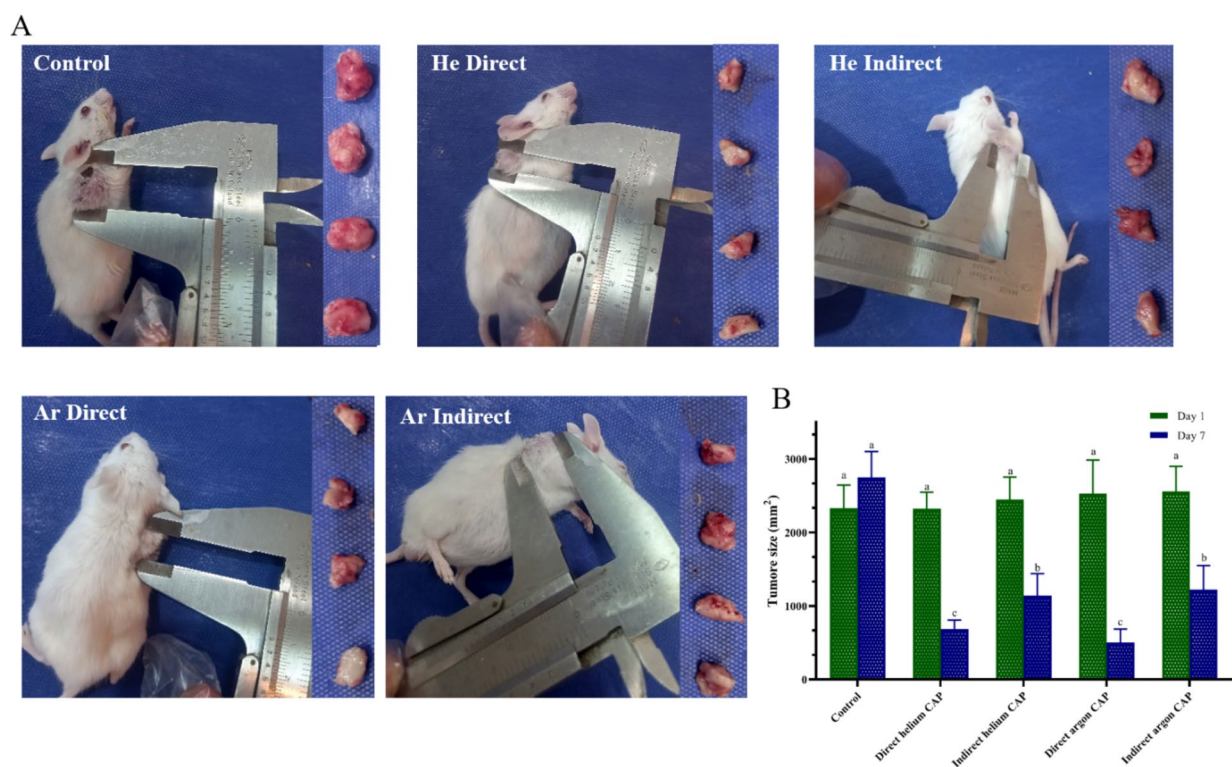


Fig. 7. (A) Schematic representation of tumor measurement by caliper on 1st day, and (B) Comparison of tumor size (mm²) in different studied groups on 1st and 7th day. * Means followed by the same letter are not significantly different ($p < 0.05$).

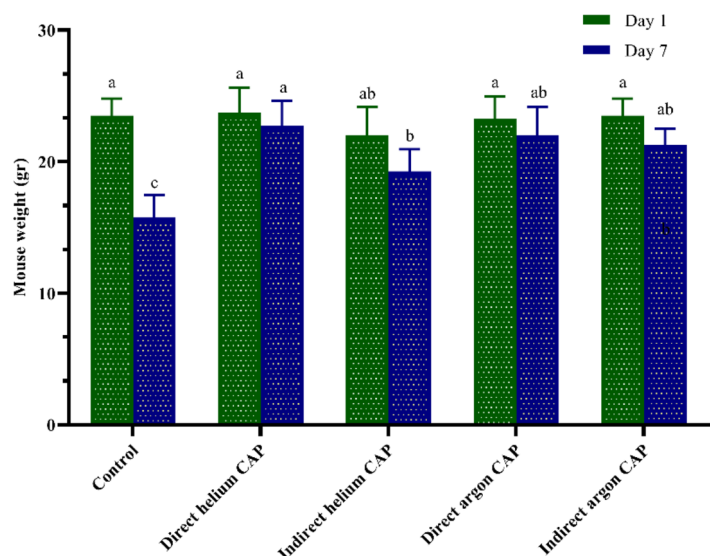


Fig. 8. The weight of mice in different studied groups on the 1st and 7th day. * Means followed by the same letter are not significantly different ($p < 0.05$).

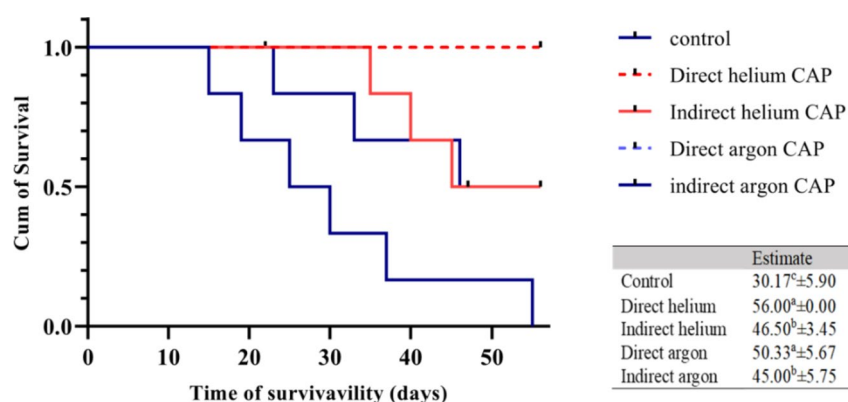


Fig. 9. Kaplan-Meier plot to analyze the difference in Mean survival time of mice treated with different plasmas therapy 8 Weeks Post-Treatment. * Means followed by the same letter are not significantly different ($p < 0.05$).

Discussion

Breast cancer is the most common cancer in women worldwide and the second cause of death from cancer. In 2020, 2.3 million women were diagnosed with breast cancer, and 685,000 deaths were recorded globally. Approved therapeutic strategies, including surgery, radiotherapy, chemotherapy, immunotherapy, hormone therapy, or a mixture of these options, are effective in cancer treatment and increase patient overall survival⁷¹. Surgery is the primary treatment due to its minimal side effects and complications. Additional therapies are used to prevent disease recurrence. Nevertheless, inherent or acquired resistance of tumor cells to cell death-induced by additional therapies and their ability to invade host tissues and metastasize to distant sites impedes therapeutic efficacy, especially in the aggressive triple-negative breast cancer molecular type^{56,72}. The increase in mortality from breast cancer and the occurrence of various severe side effects such as organ damage and reduction in overall quality of life indicate that more research is needed to find complementary or alternative therapeutic strategies⁵⁴.

CAP technology has emerged as an innovative tool for various biological and medical sciences^{73,74}. Applications of CAP in cancer therapy have been recommended for more than 15 years, leading to the establishment of a new field in medicine called “plasma oncology”. Although many studies exhibit specificity of CAP for in vitro and in vivo treatment of breast cancer, our study, for the first time, aims to compare the optimal exposure time, duration, and direct or indirect dependent effects of two CAPs based on helium and argon gases, in a triple negative cell line and an animal model of breast cancer.

Based on the calculated IC₅₀ values, the optimal exposure times were 66.52 s at the 24-hour post-treatment time point for direct helium, 110.6 s at the 48-hour post-treatment time point for indirect helium, 155 s, and

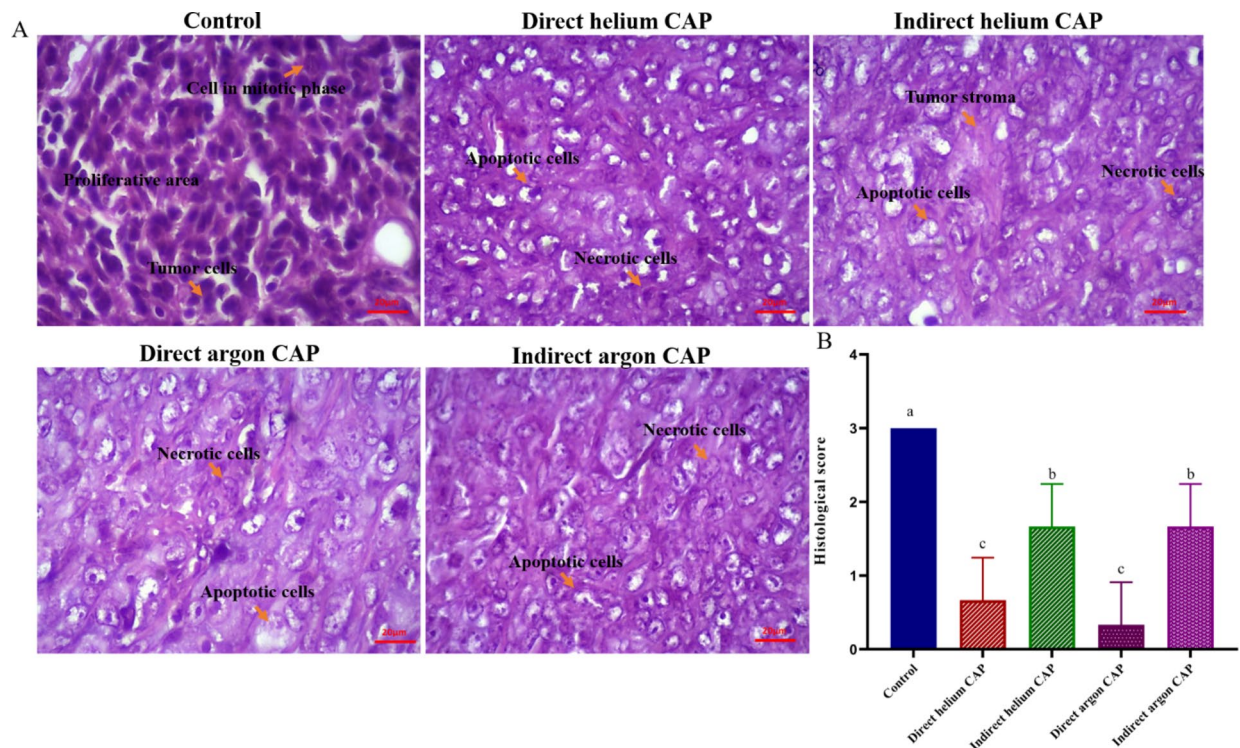


Fig. 10. (A); Tumor tissue hematoxylin and eosin (H&E) stain of five animal groups, and (B); Quantitative plot of histological score of tumor samples. * Means followed by the same letter are not significantly different ($p < 0.05$).

214.8 s at the 72-hour post-treatment time point for direct and indirect argon CAPs, respectively. These data, consistent with previous studies, revealed that CAP has time-dependent toxicity on cancer cells^{52,75,76}.

Our results also showed that CAP induces sub-G1 arrest in the 4T1 cell line and increases apoptotic cell death in direct and indirect approaches. An extensive array of plasma devices and feed gas settings was used across different studies to investigate the toxicity in breast cancer in vitro^{41,54,77–79} and in vivo^{44,80,81}. Intensive literature has focused on using helium and argon because they produce stable plasma due to their monatomic nature, chemical inertness, and lower ionization potential^{82,83}. All studies showed cytotoxic or growth-inhibiting effects of plasma in the breast cancer cell lines and an animal model of breast cancer^{40–45}. In this regard, Mirpour et al. reported that the direct helium plasma treatment reduces metastatic behavior, increases apoptosis, and delays DNA fragmentation in the sub-G1 phase of 4T1 cells⁴⁴. Although plasma therapy in direct and indirect approaches induced apoptosis, our results showed that the total apoptosis rate was higher in direct helium and direct argon groups, respectively. In confirmation of our results, many studies also report the therapeutic advantages of direct gas plasma on various molecular subtypes of breast cancer cell lines and animal models of breast cancer^{44,84–86}. While the direct application approach had the highest apoptosis rate, indirect plasma treatment also induced a significant level of apoptosis compared to the control group. Some studies aligning with our data also state that solutions activated by cold plasma can induce cancer cell apoptosis and reduce the number of metastatic nodules^{86,87}. This makes it a clinically compatible treatment modality, especially for treating less accessible tumors or those with high metastatic potential.

The precise mechanisms of CAP's oncological advantage are not completely clear; however, more research confirms that gas plasma-induced ROS/RNS, both in vitro and in vivo, are responsible for the cellular responses induced by CAP in atmospheric air or solution^{88,89}. The balance between the extent of the induced oxidative stress and the antioxidative mechanisms in the cells would render the cells toward death or survival^{72,90}. In the normal state, an antioxidant system of the cell simultaneously detoxifies ROS and maintains redox balance⁹¹. Elevated levels of reactive species produced by cold plasma disrupt redox homeostasis and induce oxidative stress^{92,93}. Consistent with the literature, our results also showed that after CAP therapy, intracellular ROS levels significantly increased, while TAC levels significantly decreased. The highest levels of ROS and the lowest levels of TAC were reported in direct helium and direct argon CAPs treated cell lines, consistent with the apoptosis rate and more potent cell cytotoxicity of the direct approach.

CAP-induced RONS initiate lipid peroxidation, compromising membrane integrity and facilitating ROS influx. This intracellular oxidative stress triggers a cascade of cellular events leading to cell death^{92,94}. It has been known that the interaction between ROS signaling and calcium signaling increases mitochondrial membrane permeability, elevating the release of cytochrome c (a key pro-apoptotic protein), and triggers the activation of apoptotic signaling in cancer cells via the mitochondrial pathway^{86,87}. Besides the interaction between ROS and

calcium signaling, ROS can cross the nuclear membrane and induce DNA damage in cancer cells, leading to cell death^{95–97}.

It is a fact that differences in ionization potential among gases lead to plasmas characterized by unique concentrations and compositions of reactive species^{6,13}. For example, the higher electron temperature of helium plasma, facilitated by its superior excitation energy and lower mass, enables efficient nitrogen ionization. In contrast, the lower metastable energy of argon limits its ionizing capacity. Additionally, the reduced electron density of helium prolongs the lifetime of excited species, enhancing NO formation^{98–101}. Although total levels of reactive species were similar between the helium and argon plasmas, the composition and concentration of these species differed significantly, which may account for the varying rates of apoptosis between the two types of plasma.

As mentioned, plasma ROS is responsible for plasma-induced cancer cell death. Various parameters control plasma jet output (ROS, UV, ozone, ion, etc.), including plasma jet source design, capillary tube geometry, gas flow characteristics, target geometry, tube-target distance, and electrical characteristics. Manipulating these parameters changes CAP composition and RONS concentration, which can cause different effects on the cancer cells¹⁰². In addition, as we know, the CAP cytotoxicity is due to short-lived species, long-lived species, and physical factors¹⁰³. It has been reported that short-lived species and physical factors after production in a medium were decreased or eliminated compared to direct treatment^{84,103}. In confirmation of our results, some studies state that the direct treatment approach is more effective than the indirect approach, emphasizing the importance of CAP-generated short-lived species and physical factors for growth inhibition and cell cytotoxicity of tumors^{85,86,103}. Since the presence of various free radicals, their concentration, and their type (long-lived or short-lived species) play crucial roles in CAP anti-cancer properties, it seems that differences in the geometry of the plasma jet, the kind of gas input, and the type of treatment approaches can change these parameters and be the possible cause of the difference in our treated groups.

In line with *in vitro* findings, plasma therapy with direct and indirect helium and argon gases significantly reduced tumor size. Tumor shrinkage in CAP-treated groups confirmed the efficacy of CAP alone in preventing breast tumor growth *in vivo*. In addition to reducing tumor size, CAP prevented weight loss and increased overall survival in all treated groups. These data, consistent with previous studies, demonstrate CAP's selective targeting of cancer cells over normal cells and its safety profile^{52,93}. Standard cancer treatments such as chemotherapy and radiotherapy target both cancer cells and healthy cells, leading to numerous side effects, including weight loss and decreased survival^{52,87}. Differences in the number of aquaporins and the amount of membrane cholesterol between malignant and non-malignant cells may explain the potential selectivity of CAP⁹⁷.

Although apoptosis induction is the main reason for the antiproliferative effect of CAP on cancer cells, reduced angiogenesis can be another possible reason for decreased tumor volume in plasma-treated groups of our study and can be considered a promising therapeutic approach of CAP in the field of oncology⁶⁴.

Our histological results showed that plasma therapy led to a significant decrease in Nottingham's histological score. The stage and grade of breast cancer tumors affect the type of treatment and prognosis. Studies confirmed that a decrease in histological score resulted in a better prognosis for breast cancer^{64,104}. The down-scoring of breast cancer and tumor size in response to plasma therapy may be promising for breast-conserving surgery instead of mastectomy in the clinical stage. The main challenge in presenting this therapeutic approach is verifying its safety. Involuntary weight loss is one of the main side effects of cancer and its treatment⁸⁷. Our results showed that plasma therapy prevented significant weight loss in all treated groups, especially in direct CAP helium and direct CAP argon groups. The lack of weight loss, along with the increased survival rate, can confirm the safety of this treatment protocol.

The potential of gas plasma for selectively targeting breast tumor cells and its safety highlight the promising potential of CAP in breast cancer therapy alone or in combination with other therapeutic protocols in the clinical stage^{105,106}. However, there are challenges for the clinical implementation of gas plasma medicine, and only a few clinical trial studies have been registered. For the first time, Canady et al. evaluated the CAP's ability to prevent tumor recurrence in a clinical trial study. The promising findings of their study demonstrated the device's ability to control residual disease and improve patient survival (Clinical Trials identifier: NCT04267575)³. Additionally, Metelmann et al. reported that direct exposure of the head and neck tumors or their bed to gas plasma has therapeutic advantages¹⁰⁷. However, more studies with a larger sample size are needed to approve CAP therapy as an approved cancer protocol.

Conclusion

For the first time, we aimed to evaluate and compare the optimal exposure time and direction-dependent cellular effects of helium and argon gas plasma on 4T1 cancer cells and a triple-negative mouse model of breast cancer. Our findings indicate that direct helium plasma treatment significantly enhanced apoptosis in 4T1 cancer cells within a shorter exposure time and also led to a higher proportion of cells arrested in the sub-G1 phase. These results, along with the reduction in tumor size and prolonged survival in animals provide a possible rationale for the clinical application of direct helium plasma. Although the direct treatment approach demonstrated higher cancer cell cytotoxicity compared to the indirect approach in our study, it may be challenging to apply deep within certain subjects. One of the greatest advantages of PAM is its potential for storage at room temperature or frozen while retaining its anti-cancer properties. This makes it a clinically compatible treatment modality, especially for treating less accessible tumors or those with high metastatic potential.

Data availability

Data used and/or analyzed in the current study are available from the corresponding author upon request.

Received: 27 September 2024; Accepted: 18 March 2025

Published online: 27 March 2025

References

1. Ma, J. & Jemal, A. Breast cancer statistics. *Breast cancer metastasis drug resistance: progress prospects* 1–18. (2013).
2. Aggelopoulos, C. A. et al. Cold atmospheric plasma attenuates breast cancer cell growth through regulation of cell microenvironment effectors. *Front. Oncol.* **11**, 5797 (2022).
3. Canady, J. et al. The first cold atmospheric plasma phase I clinical trial for the treatment of advanced solid tumors: A novel treatment arm for cancer. *Cancers (Basel)* **15**(14). (2023).
4. Chen, F. F. *Introduction to plasma physics and controlled fusion* (Springer, 1984).
5. Kikuchi, M., Lackner, K. & Tran, M. Q. *Fusion physics*. (2012).
6. Ding, T., Cullen, P. J. & Yan, W. *Applications of cold plasma in food safety* (Springer, 2022).
7. Speranza, G., Liu, W. & Minati, L. *Applications of plasma technologies to material processing* (CRC, 2019).
8. Makabe, T. & Petrovic, Z. L. *Plasma electronics: applications in microelectronic device fabrication* (CRC, 2014).
9. Misra, N., Schlüter, O. & Cullen, P. *Plasma in food and agriculture. cold plasma in food and agriculture* 1–16 (Elsevier, 2016).
10. Laroussi, M., Kong, M., Morfill, G. & Stolz, W. *Plasma medicine: applications of low-temperature gas plasmas in medicine and biology* (Cambridge University Press, 2012).
11. De Geyter, N. & Morent, R. Nonthermal plasma sterilization of living and nonliving surfaces. *Annu. Rev. Biomed. Eng.* **14**, 255–274 (2012).
12. Bernhardt, T. et al. Plasma medicine: Applications of cold atmospheric pressure plasma in dermatology. *Oxidative medicine and cellular longevity*. 2019. (2019).
13. Masur, K. *Cold plasma based wound healing application* 93–109 (Springer, 2023).
14. Glover, J., Bendick, P., Link, W. & Plunkett, R. The plasma scalpel: a new thermal knife. *Lasers Surg. Med.* **2** (1), 101–106 (1982).
15. Kwon, J.-S. *Cold plasma in dentistry. plasma biosciences and medicine* 61–76 (Springer, 2023).
16. Heslin, C. et al. Quantitative assessment of blood coagulation by cold atmospheric plasma. *Plasma Med.* **4**, 1–4 (2014).
17. Dubuc, A. et al. Use of cold-atmospheric plasma in oncology: A concise systematic review. *Therapeutic Adv. Med. Oncol.* **10**, 1758835918786475 (2018).
18. Gjika, E. et al. The cutting mechanism of the electrosurgical scalpel. *J. Phys. D.* **50** (2), 025401 (2016).
19. Shashurin, A. et al. Electric discharge during electrosurgery. *Sci. Rep.* **5** (1), 1–7 (2015).
20. Zenker, M. Argon plasma coagulation. *GMS Krankenhaushygiene Interdisziplinär* **3**(1). (2008).
21. Laroussi, M., Lu, X., Keidar, M. & Perspective The physics, diagnostics, and applications of atmospheric pressure low temperature plasma sources used in plasma medicine. *J. Appl. Phys.* **122** (2), 020901 (2017).
22. Kalghatgi, S. et al. (eds) On the interaction of non-thermal atmospheric pressure plasma with tissues. *IEEE Pulsed Power Conference*; 2009: IEEE. (2009).
23. Barton, A. et al. (eds) Non-thermal atmospheric pressure plasma treatment of human cells: the effect of ambient conditions. *Proceedings of 21st International Symposium on Plasma Chemistry* (4–9 August 2013, Cairns, Australia); (2013).
24. Hara, H. & Adachi, T. Molecular mechanisms of non-thermal atmospheric pressure plasma-induced cellular responses. *Jpn. J. Appl. Phys.* **60** (2), 020501 (2021).
25. Song, K., Li, G. & Ma, Y. A review on the selective apoptotic effect of nonthermal atmospheric-pressure plasma on cancer cells. *Plasma Med.* **4**, 1–4 (2014).
26. Ma, Y. et al. Non-thermal atmospheric pressure plasma preferentially induces apoptosis in p53-mutated cancer cells by activating ROS stress-response pathways. *PLoS One.* **9** (4), e91947 (2014).
27. Kim, C.-H. et al. Induction of cell growth arrest by atmospheric non-thermal plasma in colorectal cancer cells. *J. Biotechnol.* **150** (4), 530–538 (2010).
28. Vandamme, M. et al. (eds) In situ application of non-thermal plasma: preliminary investigations for colorectal and lung tolerance. *Proceedings of the International Symposium on Plasma Chemistry* (ISPC-20); (2011).
29. Weltmann, K.-D., Metelmann, H.-R. & Von Woedtke, T. Low temperature plasma applications in medicine. *Europhys. News.* **47** (5–6), 39–42 (2016).
30. Khanikar, R. R. & Bailung, H. *Cold atmospheric pressure plasma technology for biomedical application* (Plasma Science and Technology, 2022).
31. Isbary, G. et al. Cold atmospheric plasma devices for medical issues. *Expert Rev. Med. Dev.* **10** (3), 367–377 (2013).
32. Rehman, M. U. et al. Physical and chemical enhancement of cancer cell death induced by cold atmospheric plasma. *Jpn. J. Appl. Phys.* **60** (3), 030501 (2021).
33. Graves, D. B. Reactive species from cold atmospheric plasma: implications for cancer therapy. *Plasma Processes Polym.* **11** (12), 1120–1127 (2014).
34. Yan, D. et al. The cell activation phenomena in the cold atmospheric plasma cancer treatment. *Sci. Rep.* **8** (1), 1–10 (2018).
35. Xu, D. et al. NO₂- and NO₃-enhance cold atmospheric plasma induced cancer cell death by generation of ONOO. *AIP Adv.* **8** (10), 105219 (2018).
36. Wang, Q. et al. A comparative study of cold atmospheric plasma treatment, chemical versus physical strategy. *J. Phys. D.* **54** (9), 095207 (2020).
37. Boeckmann, L. et al. Cold atmospheric pressure plasma in wound healing and cancer treatment. *Appl. Sci.* **10** (19), 6898 (2020).
38. Jawaid, P. et al. Helium-based cold atmospheric plasma-induced reactive oxygen species-mediated apoptotic pathway attenuated by platinum nanoparticles. *J. Cell. Mol. Med.* **20** (9), 1737–1748 (2016).
39. Radmilovic-Radjenovic, M., Radjenovic, B., Bojarov, A., Klas, M. & Matejcik, S. The breakdown mechanisms in electrical discharges: the role of the field emission effect in direct current discharges in micro gaps. *Acta Phys. Slovaca* **63**. (2013).
40. Chen, Z. et al. Micro-sized cold atmospheric plasma source for brain and breast cancer treatment. *Plasma Med.* **8**(2). (2018).
41. Cheng, X. et al. Treatment of triple-negative breast cancer cells with the Canady cold plasma conversion system: preliminary results. *Plasma* **1** (1), 218–228 (2018).
42. Cheng, X. et al. Canady helios cold plasma induces breast cancer cell death by oxidation of histone mRNA. *Int. J. Mol. Sci.* **22** (17), 9578 (2021).
43. Boisvert, J.-S., Lafontaine, J., Glory, A., Coulombe, S. & Wong, P. Comparison of three radio-frequency discharge modes on the treatment of breast cancer cells in vitro. *IEEE Trans. Radiation Plasma Med. Sci.* **4** (5), 644–654 (2020).
44. Mirpour, S. et al. Utilizing the micron sized non-thermal atmospheric pressure plasma inside the animal body for the tumor treatment application. *Sci. Rep.* **6** (1), 29048 (2016).
45. Mehrabifard, R., Mehdian, H. & Bakhshzadmahmoudi, M. Effect of non-thermal atmospheric pressure plasma on MDA-MB-231 breast cancer cells. R Mehrabifard, H Mehdian, and Mahdi Bakhshzadmahmoudi, Effect of non-thermal atmospheric pressure plasma on MDA-MB-231 breast cancer cells. *Pharm. Biomed. Res.* **3** (3), 12–16 (2017).
46. Kim, S. J., Chung, T., Bae, S. & Leem, S. Induction of apoptosis in human breast cancer cells by a pulsed atmospheric pressure plasma jet. *Appl. Phys. Lett.* **97** (2), 023702 (2010).
47. Georgescu, N. & Lupu, A. R. Tumoral and normal cells treatment with high-voltage pulsed cold atmospheric plasma jets. *IEEE Trans. Plasma Sci.* **38** (8), 1949–1955 (2010).

48. Mirpour, S. et al. The selective characterization of nonthermal atmospheric pressure plasma jet on treatment of human breast cancer and normal cells. *IEEE Trans. Plasma Sci.* **42** (2), 315–322 (2014).
49. Chen, Z. et al. A novel micro cold atmospheric plasma device for glioblastoma both in vitro and in vivo. *Cancers* **9** (6), 61 (2017).
50. Arndt, S. et al. Cold atmospheric plasma, a new strategy to induce senescence in melanoma cells. *Exp. Dermatol.* **22** (4), 284–289 (2013).
51. Zucker, S. N. et al. Preferential induction of apoptotic cell death in melanoma cells as compared with normal keratinocytes using a non-thermal plasma torch. *Cancer Biol. Ther.* **13** (13), 1299–1306 (2012).
52. Bakhtiyari-Ramezani, M. et al. Comparative assessment of direct and indirect cold atmospheric plasma effects, based on helium and Argon, on human glioblastoma: an in vitro and in vivo study. *Sci. Rep.* **14** (1), 3578 (2024).
53. Pulaski, B. A. & Ostrand-Rosenberg, S. Mouse 4T1 breast tumor model. *Curr. Protocols Immunol.* **39** (1), 20 (2000). 1–2. 16.
54. Bekeschus, S., Saadati, F. & Emmert, S. The potential of gas plasma technology for targeting breast cancer. *Clin. Translational Med.* **12** (8), e1022 (2022).
55. Nedeljković, M. & Damjanović, A. Mechanisms of chemotherapy resistance in triple-negative breast cancer—how we can rise to the challenge. *Cells* **8** (9), 957 (2019).
56. Bai, X., Ni, J., Beretov, J., Graham, P. & Li, Y. Triple-negative breast cancer therapeutic resistance: where is the Achilles' heel? *Cancer Lett.* **497**, 100–111 (2021).
57. Tavares-da-Silva, E. et al. Cold atmospheric plasma, a novel approach against bladder cancer, with higher sensitivity for the high-grade cell line. *Biology* **10** (1), 41 (2021).
58. Welz, C. et al. Cold atmospheric plasma: a promising complementary therapy for squamous head and neck cancer. *PLoS One.* **10** (11), e0141827 (2015).
59. Wang, X. et al. Chemotherapeutic drugs stimulate the release and recycling of extracellular vesicles to assist cancer cells in developing an urgent chemoresistance. *Mol. Cancer.* **18**, 1–18 (2019).
60. He, Y. et al. The changing 50% inhibitory concentration (IC50) of cisplatin: a pilot study on the artifacts of the MTT assay and the precise measurement of density-dependent chemoresistance in ovarian cancer. *Oncotarget* **7** (43), 70803 (2016).
61. Lee, M. C., Chen, Y. K., Hsu, Y. J. & Lin, B. R. Niclosamide inhibits the cell proliferation and enhances the responsiveness of esophageal cancer cells to chemotherapeutic agents. *Oncol. Rep.* **43** (2), 549–561 (2020).
62. He, Y. et al. The changing 50% inhibitory concentration (IC50) of cisplatin: a pilot study on the artifacts of the MTT assay and the precise measurement of density-dependent chemoresistance in ovarian cancer. *Oncotarget* **7** (43), 70803–70821 (2016).
63. Rajaratnam, H. et al. Passage number of 4T1 cells influences the development of tumour and the progression of metastasis in 4T1 orthotopic mice. *Malaysian J. Med. Sciences: MJMS.* **29** (3), 30 (2022).
64. Takahashi, H. et al. Molecular biological features of Nottingham histological grade 3 breast cancers. *Ann. Surg. Oncol.* **27**, 4475–4485 (2020).
65. Jaiswal, S. & Aguirre, E. Comparison of atmospheric pressure argon producing O (1S) and helium plasma jet on methylene blue degradation. *AIP Adv.* **11**(4). (2021).
66. Jamil, M. et al. Atmospheric pressure glow discharge (APGD) plasma generation and surface modification of aluminum and Silicon Si (100). *Digest J. Nanomaterials Biostructures.* **12**, 595–604 (2017).
67. Zaplotnik, R., Primc, G. & Vesel, A. Optical emission spectroscopy as a diagnostic tool for characterization of atmospheric plasma jets. *Appl. Sci.* **11** (5), 2275 (2021).
68. Jeon, S. U., Kim, J. W., Lee, H.-Y., Kim, G.-C. & Lee, H. J. Characteristics of merging plasma plumes for materials process using two atmospheric pressure plasma jets. *Materials* **17** (19), 4928 (2024).
69. Lamichane, P. et al. Non-thermal argon plasma jets of various lengths for selective reactive oxygen and nitrogen species production. *J. Environ. Chem. Eng.* **10** (3), 107782 (2022).
70. Veda Prakash, G., Behera, N., Patel, K. & Kumar, A. Concise characterization of cold atmospheric pressure helium plasma jet. *AIP Adv.* **11**(8). (2021).
71. Haralambiev, L. et al. Inhibition of angiogenesis by treatment with cold atmospheric plasma as a promising therapeutic approach in oncology. *Int. J. Mol. Sci.* **21** (19), 7098 (2020).
72. Rana, J. N., Mumtaz, S., Han, I. & Choi, E. H. Harnessing the synergy of nanosecond high-power microwave pulses and cisplatin to increase the induction of apoptosis in cancer cells through the activation of ATR/ATM and intrinsic pathways. *Free Radic. Biol. Med.* **225**, 221–235 (2024).
73. Yousfi, M., Merbahi, N., Pathak, A. & Eichwald, O. Low-temperature plasmas at atmospheric pressure: toward new pharmaceutical treatments in medicine. *Fundam Clin. Pharmacol.* **28** (2), 123–135 (2014).
74. Cheng, X. et al. The effect of tuning cold plasma composition on glioblastoma cell viability. *PLoS One.* **9** (5), e98652 (2014).
75. Min, T. et al. Therapeutic effects of cold atmospheric plasma on solid tumor. *Front. Med.* **9**, 884887 (2022).
76. Babajani, A. et al. Reactive oxygen species from non-thermal gas plasma (CAP): implication for targeting cancer stem cells. *Cancer Cell Int.* **24** (1), 344 (2024).
77. Nagaya, M., Hara, H., Kamiya, T. & Adachi, T. Inhibition of NAMPT markedly enhances plasma-activated medium-induced cell death in human breast cancer MDA-MB-231 cells. *Arch. Biochem. Biophys.* **676**, 108155 (2019).
78. Lin, A. et al. Non-thermal plasma as a unique delivery system of short-lived reactive oxygen and nitrogen species for Immunogenic cell death in melanoma cells. *Adv. Sci.* **6** (6), 1802062 (2019).
79. Bekeschus, S. et al. xCT (SLC7A11) expression confers intrinsic resistance to physical plasma treatment in tumor cells. *Redox Biol.* **30**, 101423 (2020).
80. Xiang, L., Xu, X., Zhang, S., Cai, D. & Dai, X. Cold atmospheric plasma conveys selectivity on triple negative breast cancer cells both in vitro and in vivo. *Free Radic. Biol. Med.* **124**, 205–213 (2018).
81. Mahdikia, H. et al. Gas plasma irradiation of breast cancers promotes immunogenicity, tumor reduction, and an abscopal effect in vivo. *Oncoimmunology* **10** (1), 1859731 (2021).
82. Stoffels, E., Flikweert, A., Stoffels, W. & Kroesen, G. Plasma needle: a non-destructive atmospheric plasma source for fine surface treatment of (bio) materials. *Plasma Sources Sci. Technol.* **11** (4), 383 (2002).
83. Kim, S. J., Chung, T., Bae, S. & Leem, S. Induction of apoptosis in human breast cancer cells by a pulsed atmospheric pressure plasma jet. *Appl. Phys. Lett.* **97**(2). (2010).
84. Stańczyk, B. & Wiśniewski, M. The promising potential of cold atmospheric plasma therapies. *Plasma* **7** (2), 465–497 (2024).
85. Mashayekh, S., Rajae, H., Akhlaghi, M., Shokri, B. & Hassan, Z. M. Atmospheric-pressure plasma jet characterization and applications on melanoma cancer treatment (B/16-F10). *Phys. Plasmas* **22**(9). (2015).
86. Malyavko, A. et al. Cold atmospheric plasma cancer treatment, direct versus indirect approaches. *Mater. Adv.* **1** (6), 1494–1505 (2020).
87. Rolim, G. B. et al. Can inflammasomes promote the pathophysiology of glioblastoma multiforme? A view about the potential of the anti-inflammasome therapy as Pharmacological target. *Crit. Rev. Oncol. /Hematol.* **172**, 103641 (2022).
88. Keidar, M., Yan, D., Beilis, I. I., Trink, B. & Sherman, J. H. Plasmas for treating cancer: opportunities for adaptive and Self-Adaptive approaches. *Trends Biotechnol.* **36** (6), 586–593 (2018).
89. Khalili, M. et al. Non-Thermal Plasma-Induced Immunogenic cell death in cancer: A topical review. *J. Phys. D Appl. Phys.* **52**(42). (2019).
90. Bhattacharyya, A., Chattopadhyay, R., Mitra, S. & Crowe, S. E. Oxidative stress: an essential factor in the pathogenesis of Gastrointestinal mucosal diseases. *Physiol. Rev.* **94** (2), 329–354 (2014).

91. He, L. et al. Antioxidants maintain cellular redox homeostasis by elimination of reactive oxygen species. *Cell. Phys. Biochem.* **44** (2), 532–553 (2017).
92. Mateu-Sanz, M., Tornín, J., Ginebra, M.-P. & Canal, C. Cold atmospheric plasma: a new strategy based primarily on oxidative stress for osteosarcoma therapy. *J. Clin. Med.* **10** (4), 893 (2021).
93. Rezaeinezhad, A., Eslami, P., Mirmiranpour, H. & Ghomi, H. The effect of cold atmospheric plasma on diabetes-induced enzyme glycation, oxidative stress, and inflammation; in vitro and in vivo. *Sci. Rep.* **9** (1), 19958 (2019).
94. Turrini, E. et al. Cold atmospheric plasma induces apoptosis and oxidative stress pathway regulation in T-lymphoblastoid leukemia cells. *Oxidative Med. Cell. Longev.* **2017** (1), 4271065 (2017).
95. Brány, D. et al. Effect of cold atmospheric plasma on epigenetic changes, DNA damage, and possibilities for its use in synergistic cancer therapy. *Int. J. Mol. Sci.* **22** (22), 12252 (2021).
96. Gaur, N. et al. On cold atmospheric-pressure plasma jet induced DNA damage in cells. *J. Phys. D: Appl. Phys.* **54** (3), 035203 (2020).
97. Semmler, M., Bekeschus, S. & Schäfer, M. Molecular mechanisms of the efficacy of cold atmospheric pressure plasma (CAP) in cancer treatment. *Cancers* **12**, 269 (2020).
98. Jonkers, J., Van De Sande, M., Sola, A., Gamero, A. & Van Der Mullen, J. On the differences between ionizing helium and argon plasmas at atmospheric pressure. *Plasma Sources Sci. Technol.* **12** (1), 30 (2002).
99. Seo, Y. S. et al. Comparative studies of atmospheric pressure plasma characteristics between he and ar working gases for sterilization. *IEEE Trans. Plasma Sci.* **38** (10), 2954–2962 (2010).
100. Motomura, H., Matsuba, H., Kawata, M. & Jinno, M. Gas-specific characteristics of argon low-frequency atmospheric-pressure nonequilibrium Microplasma jet. *Japanese J. Appl. Phys.* **46** (10L), L939 (2007).
101. Korolov, I. et al. Helium metastable species generation in atmospheric pressure RF plasma jets driven by tailored voltage waveforms in mixtures of he and N₂. *J. Phys. D: Appl. Phys.* **53** (18), 185201 (2020).
102. Viegas, P. et al. Physics of plasma jets and interaction with surfaces: review on modelling and experiments. *Plasma Sources Sci. Technol.* **31** (5), 053001 (2022).
103. Privat-Maldonado, A., Gorbanev, Y., Dewilde, S., Smits, E. & Bogaerts, A. Reduction of human glioblastoma spheroids using cold atmospheric plasma: the combined effect of short- and long-lived reactive species. *Cancers* **10** (11), 394 (2018).
104. Elston, C. W. & Ellis, I. O. Pathological prognostic factors in breast cancer. I. The value of histological grade in breast cancer: experience from a large study with long-term follow-up. *Histopathology* **19** (5), 403–410 (1991).
105. Privat-Maldonado, A., Bengtson, C., Razzokov, J., Smits, E. & Bogaerts, A. Modifying the tumour microenvironment: challenges and future perspectives for anticancer plasma treatments. *Cancers* **11** (12), 1920 (2019).
106. Graves, D. B. The emerging role of reactive oxygen and nitrogen species in redox biology and some implications for plasma applications to medicine and biology. *J. Phys. D: Appl. Phys.* **45** (26), 263001 (2012).
107. Metelmann, H.-R. et al. Clinical experience with cold plasma in the treatment of locally advanced head and neck cancer. *Clin. Plasma Med.* **9**, 6–13 (2018).

Acknowledgements

The authors would like to thank all those who generously helped in designing, conducting, interpreting the results and writing the article of this study.

Author contributions

Conceptualization and design, investigation, methodology, project administration and supervision of the study were performed by Mahdijeh Bakhtiyari Ramezani. Material preparation, data collection and analysis were performed by Mesam Nasiri, and Mansoureh Baniyasi. The original draft was written by Mansoureh Baniyasi. The authors read and approved the final manuscript.

Declarations

Competing interests

The authors declare no competing interests.

Ethical declaration

All animal procedures were done under the ethical guidelines for working with animals, were approved by the ethics committee of Shahid Beheshti University of Medical Sciences (IR.SBMU.CRC.REC.1401.039), and performed in line with the ARRIVE guidelines.

Additional information

Correspondence and requests for materials should be addressed to M.B.-R.

Reprints and permissions information is available at www.nature.com/reprints.

Publisher's note Springer Nature remains neutral with regard to jurisdictional claims in published maps and institutional affiliations.

Open Access This article is licensed under a Creative Commons Attribution-NonCommercial-NoDerivatives 4.0 International License, which permits any non-commercial use, sharing, distribution and reproduction in any medium or format, as long as you give appropriate credit to the original author(s) and the source, provide a link to the Creative Commons licence, and indicate if you modified the licensed material. You do not have permission under this licence to share adapted material derived from this article or parts of it. The images or other third party material in this article are included in the article's Creative Commons licence, unless indicated otherwise in a credit line to the material. If material is not included in the article's Creative Commons licence and your intended use is not permitted by statutory regulation or exceeds the permitted use, you will need to obtain permission directly from the copyright holder. To view a copy of this licence, visit <http://creativecommons.org/licenses/by-nc-nd/4.0/>.

© The Author(s) 2025